

MONTE CARLO STUDIES OF HUBBARD MODELS

Helen Craig

ABSTRACT

This summer, I studied two variations of the extended Hubbard model: the extended Hubbard-Holstein model and the extended Hubbard model with staggered potential. My goal was to write programs for these two models, to test these programs for accuracy, and then to derive a phase diagram from the data that these programs would produce. The technique that I used was the world line quantum Monte Carlo method.

BACKGROUND

For many years, the Hubbard model has been studied both for its simplicity and for its complexity, along with its versatility. The Hubbard model in its simplest form is a one dimension chain of atoms with one orbital each. Each of these orbitals is allowed two electrons, one up spin electron and one down spin electron. The purest form of the Hubbard model has been studied extensively. But as mentioned earlier, the Hubbard model is adaptable in simulating many different materials with a variety of properties. Among these “flavors”, we studied this summer the Hubbard-Holstein model and the Hubbard model with staggered potential.

The extended Hubbard model has an energy of

$$-t\sum_{i,\sigma}(c_{i,\sigma}^\dagger c_{i+1,\sigma} + \text{H.c.}) + U\sum_i(n_i^* n_i) + V\sum_i(n_{i+n_i})^*(n_{i+1} + n_{i+1}),$$

where $-t\sum_{i,\sigma}(c_{i,\sigma}^\dagger c_{i+1,\sigma} + \text{H.c.})$ is the component from the kinetic energy of the hopping

electrons; $U \sum_i (n_{i\uparrow} n_{i\downarrow})$ is the energy from onsite electrons; and $V \sum_i (n_{i+\uparrow} n_{i+\downarrow})$ is the energy from near neighbor electrons. i is the index of summation and the spatial site of the atom, $n_{i\downarrow}$ is the down spin electron on atom i , $n_{i\uparrow}$ is the up spin electron on atom i . If there are no up spin (down spin) electrons on the atom, then $n_{i\uparrow}$ ($n_{i\downarrow}$) is equal to zero. If the spatial site is occupied by an up spin (down spin) electron, then $n_{i\uparrow}$ ($n_{i\downarrow}$) is equal to one.

The staggered potential has an energy of $\Delta \sum_i (-1)^i (n_{i+\uparrow} n_{i+\downarrow})$. This energy is similar to the energy from V (intersite repulsion). The major difference between these energies is that where the energy $V \sum_i (n_{i+\uparrow} n_{i+\downarrow})$ has highest energy when two electrons are sitting on the same site with a near neighbor atom that also has two electrons ($E=4V$) and low energy if one orbital is empty no matter the number of electrons on the other orbitals ($E=0$); the staggered energy, on the other hand, has high energy if a even space is occupied by two electrons ($E=2\Delta$), lower energy if no electrons are in the orbital ($E=0$) and lower still energy if there are two electron on an odd space orbital ($E=-2\Delta$). What this model physically represents is a material made of two different types of atoms. These atoms alternate between even and odd sites. The odd sites have the atoms that are more metallic which explains why the electrons prefer to be on these atoms.

The Hubbard-Holstein model represents a lattice that has become distorted. The Hubbard-Holstein model is more complicated than the staggered potential and has three components to its energy. The Holstein model, in its simplest form is a lattice of atoms with a phonon sitting on each atom where a phonon is just a quantized representation of the lattice distortion. The atom and phonon are similar to a mass on a spring system

where the atom is the mass and the phonon is the spring. The energy is given by:

$$\sum \frac{1}{2} m (\dot{x}_t)^2 + \frac{1}{2} m \left[\frac{(x_t - x_{t-1})}{\beta/L} \right]^2$$

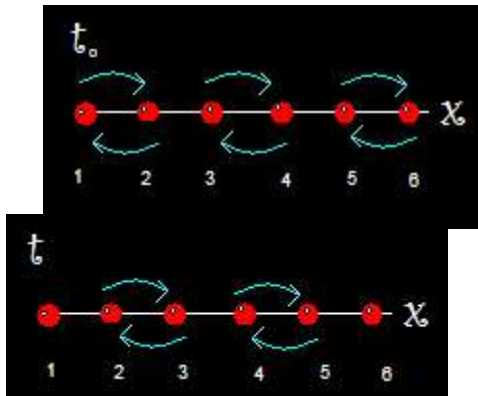
where the first part is the potential energy and the second part is the kinetic energy. m is the mass of the atom, x is the amount of distortion or the phonon, ω is the angular velocity, β is the inverse temperature and the amount of total imaginary time, L is the number of time slices and t is the index of summation and the time site.

When electrons are also included in the system, an additional component of the energy is included that couples the electrons to the phonons. This addition is $\lambda \sum x_t (n_{i+1} - n_{i-1})$ where λ is the el-ph coupling.

TECHNIQUE

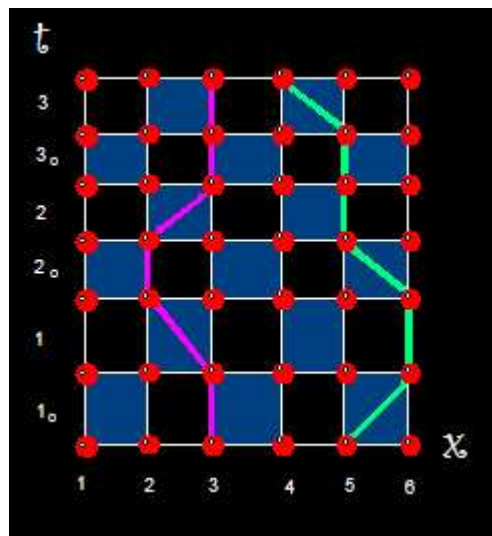
The method that we used to study our models is the world line quantum Monte Carlo method. This version of Monte Carlo method is unique for its use of imaginary time as a second dimension in addition to space. This method also uses world lines to express the hopping of the electrons where world lines can be defined simply as lines on a time-space graph, which denotes the progression of events.

So in the WLQMC method in addition the spatial dimensions is a dimension of imaginary time. For every point of time there are two time slices on the Monte Carlo grid. During the first time slice the electrons are allowed to hop between atoms 1 and 2, 3 and 4, etc.



During the second time slice, the electrons are allowed to hop between atoms 2 and 3, 4 and 5, etc.

This division gives rise to a checkerboard pattern which the electrons are allowed to cross every other square on the board (the blue squares).

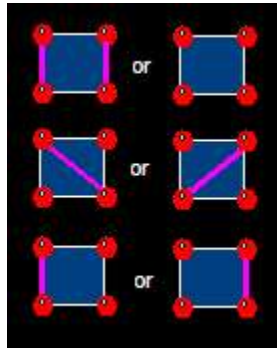


The world lines connect the electrons in the space/imaginary time grid and reveal the hopping of the electrons. The allowed moves are called pulling the world lines.

Essentially, the move suggests that an electron is moved so that it sits on an atom next to its current location during the duration of some time slice. The world line is translated

over in two locations: at the beginning of the time slice and at the end of the time slice.

The hopping kinetic energy and probability from the hopping kinetic energy is calculated depending on the way that the world lines vertically transverse the squares that they are allowed to hop across. If no world lines or two world lines are on the square, the KE is zero and the probability is one. If a single world line runs across the square, the KE is $\tanh(t*B/L)$ and the probability is $\cosh(t*B/L)$. If a single world line runs down the side of the square, the KE is $\coth(t*B/L)$ and the probability is $\sinh(t*B/L)$.



CALCULATIONS / RESULTS

The majority of results that have been obtained from the WLQMC programs are a number of checks. Some of these checks involved setting a few of the variables to zero and comparing the WLQMC data to that of other approaches such as Lanczos method and exact diagonalization. The world line quantum Monte Carlo program, in addition to finding the different energies of the system, calculates the spin density wave, the charge density wave, the spin density wave susceptibility and the charge density wave susceptibility.

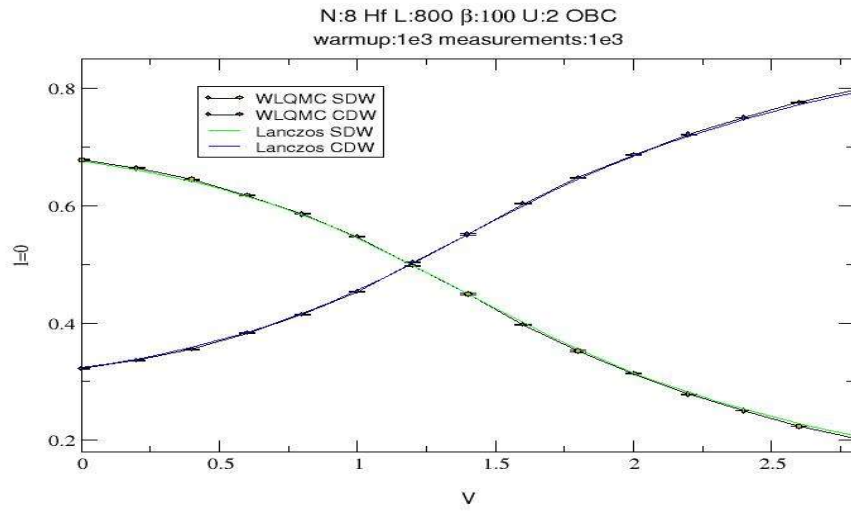


Figure Number range FigureWLQMC vs. Lanczos: CDW and SDW for $l=0$ using OBC

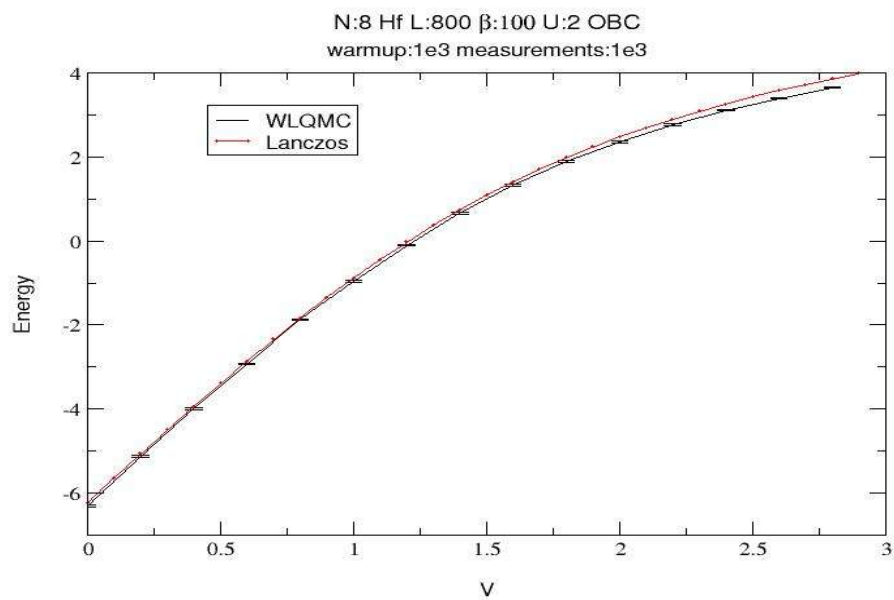


Figure Number range Figure WLQMC vs. Lanczos: Energy for Extended Hubbard Model with OBC

Figures 1 and 2 were produced as a test run for the Hubbard model without the staggered potential and without the phonons. Both the Lanczos values and the WLQMC

data were obtained using open boundary condition to make the two systems more comparative to each other. The Lanczos has a temperature of zero and the WLQMC was run for temperature equal to .01.

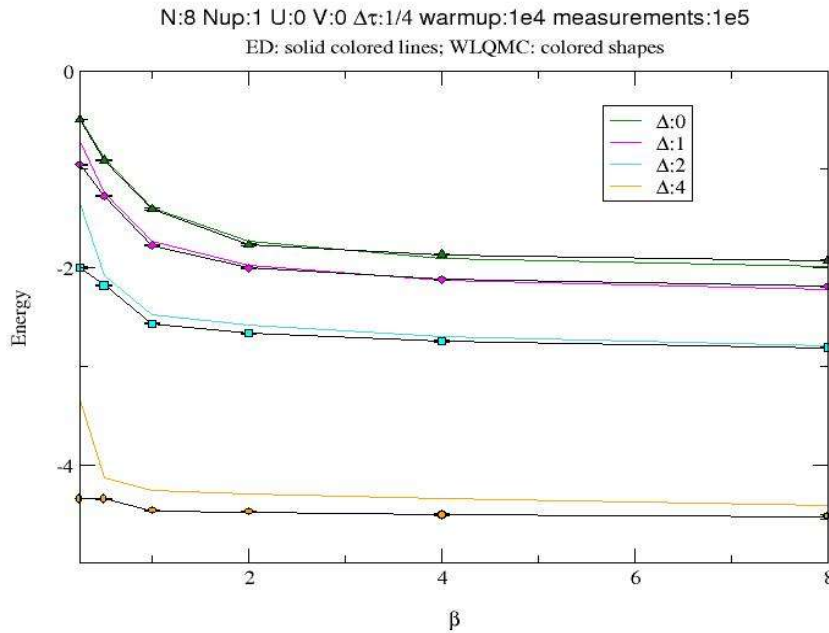


Figure Number range Figure WLQMC vs. ED: the energy for one electron at $V=U=0$ for $\Delta=0, 1, 2, 4$

Figure 3 is a comparison between the WLQMC data and data obtained by exact diagonalization for the staggered potential. Both programs were run for one electron on an eight-site lattice. For small Δ and large β , the data seemed to agree the best.

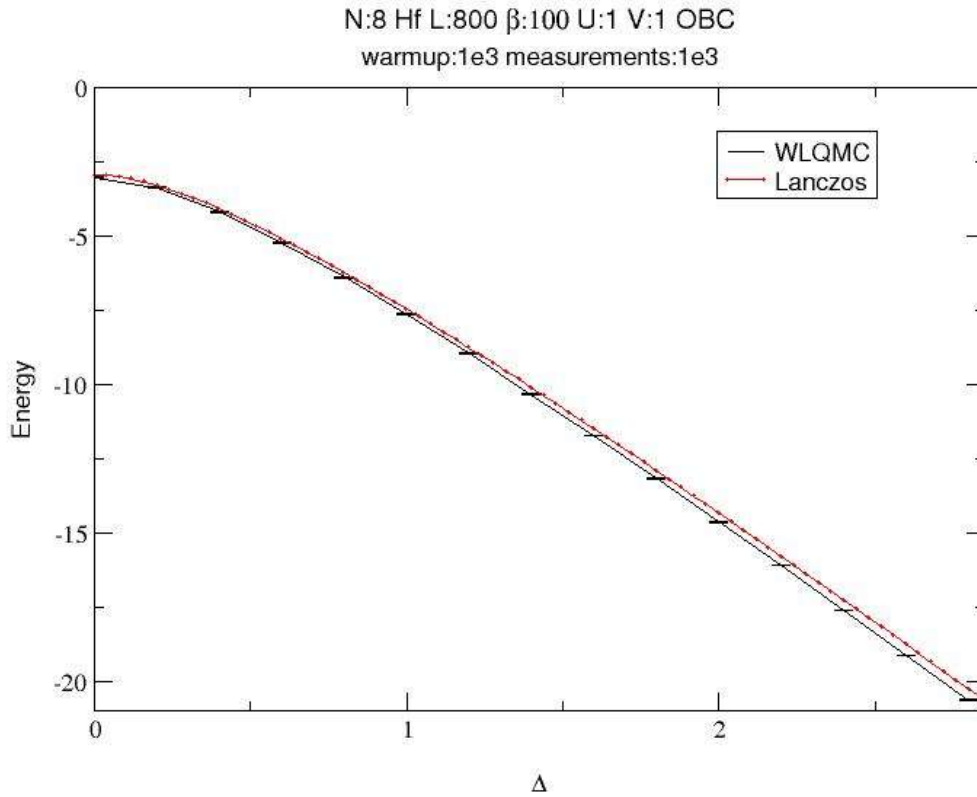


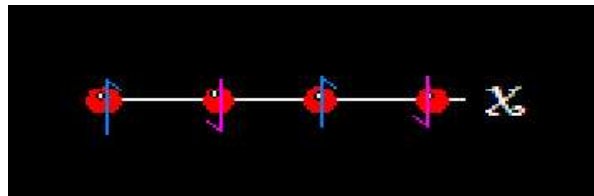
Figure Number range Figure WLQMC vs. Lanczos: Energy for the extended Hubbard model with staggered potential using OBC

Figure 4 also illustrates the accuracy of the WLQMC method with staggered potential compared to the Lanczos method. Both methods were utilized with open boundary conditions so as to make them as similar as possible. The temperature in the WLQMC simulation was .01 while the Lanczos was for temperature of zero.

The spin density wave is defined by: $SDW(j) = 1/(N*L) * \sum (n_{i-n} - n_i) * (n_{i+j-n} - n_{i+j})$;
 And the charge density wave is defined by $CDW(j) = 1/(N*L) * \sum (n_{i+n} - n_{i-1}) * (n_{i+j+n} - n_{i+j-1})$ where j is the number of spatial sites over from atom i; The susceptibility of the spin density wave is defined by:

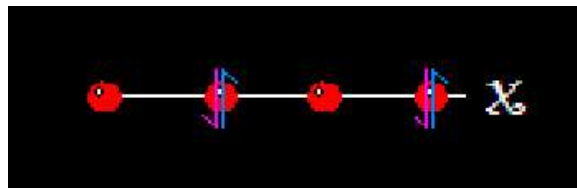
$\chi_{SDW}(j) = 1/(N \cdot L) \cdot \sum \sum \sum \sum (n_{i,k-n} - n_{i,k}) \cdot (n_{i+j,k+m-n} - n_{i+j,k+m})$; and the susceptibility of the charge density wave is defined by: $\chi_{CDW}(j) = 1/(N \cdot L) \cdot \sum \sum \sum \sum (n_{i,k} + n_{i,k} - 1) \cdot (n_{i+j,k+m} + n_{i+j,k+m} - 1)$; where k is the time site of the atom and m is the number of time sites up from time k . The variables $i, j, k,$ and m are all indexes of summation. The susceptibility of the spin density wave is a measurement of how susceptible a system is to be in the SDW phase and the susceptibility of the charge density wave is how susceptible a system is to be in the CDW phase.

If U is large, there will be a strong onsite repulsion and the following configuration will result:



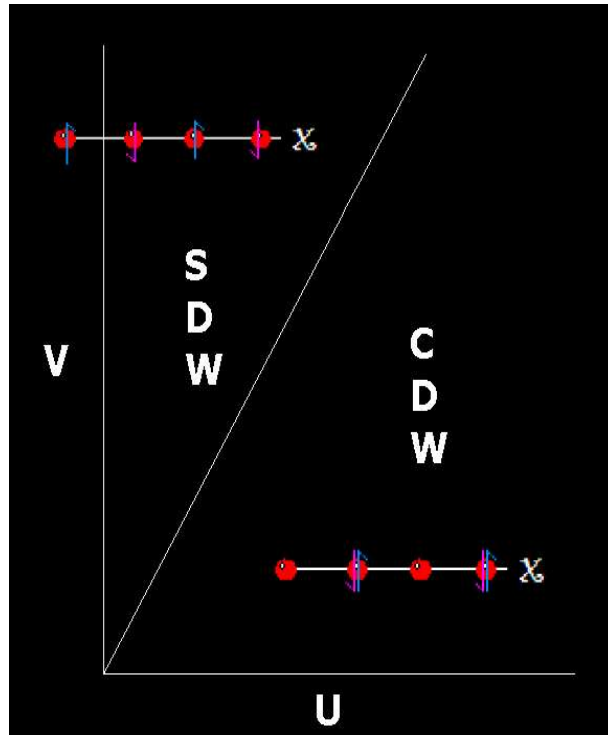
The energy per site of this system will be equal to V . Because of the up spin-down spin-up spin-down spin pattern, this phase is called the spin density wave phase.

If V is large, there will be a strong intersite repulsion and the following configuration will result:



The energy per site of this system will be equal to $U/2$. Because of the charge-no charge-charge-no charge pattern, this phase is called the charge density wave phase.

The phase transition between these two phases occurs when $V=U/2$.



When Δ or λ is nonzero, the phase transition no longer will fall upon this line. The calculations of χ_{SDW} and χ_{CDW} help to locate the point where the system has been transformed from SDW phase to CDW phase or vice versa if one of the variables V, U, Δ or λ is increased as a function of χ_{SDW} and χ_{CDW} . If the system is dominated by the up spin-down spin-up spin-down spin pattern, the susceptibility of spin density wave will be large. Conversely, if the system is dominated by the charge-no charge-charge-no charge pattern, the susceptibility of charge density wave will be large.

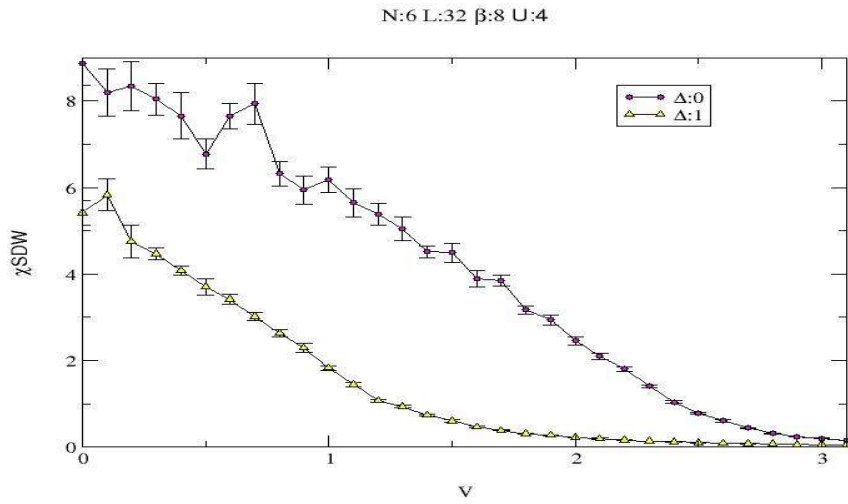


Figure Number range Figure The susceptibility of SDW for $\Delta=0, 1$

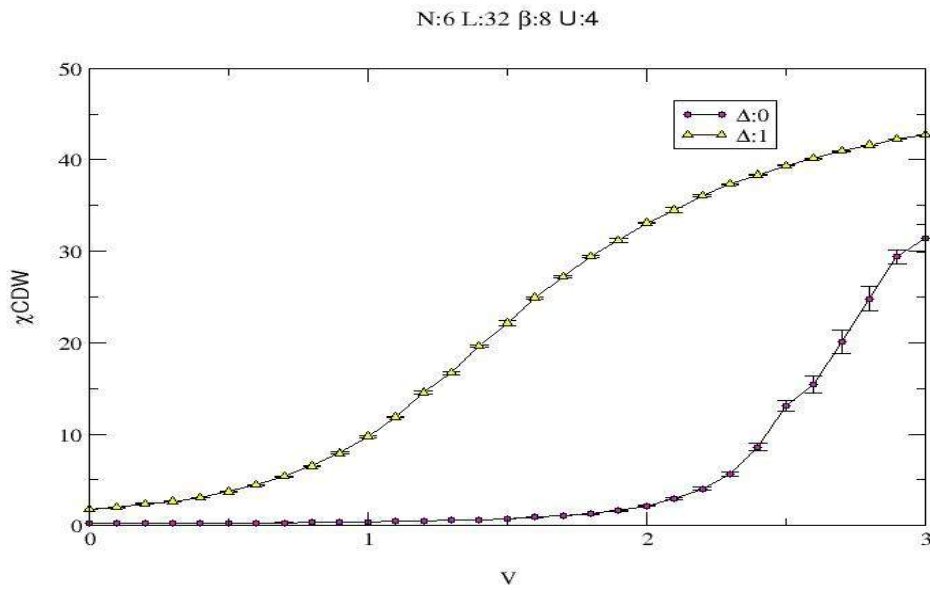


Figure Number range Figure The susceptibility of CDW for $\Delta=0, 1$

Figures 5 and 6 show the susceptibilities for CDW and SDW for $\Delta=0$ and 1. Without the hopping parameter, we predicted that the phase transition would occur at $V=U/2-\Delta$. In other words, as we turned delta on, we expected the charge density wave to

be invoked and for the spin density wave to be suppressed. This is exactly what these graphs reflect although not necessarily according to the equation since the inclusion of the hopping term, t .

A technique that we just began to utilize is finite size scaling. In an infinite system (the number of spatial sites is equal to infinity) $\chi(y)=(y-y_c)^\gamma$ where $y=V, U, \Delta$, or λ , y_c is the critical point, and $\chi = \chi_{SDW}$ or χ_{CDW} . If the spatial sites are finite, another related equation applies given by $\chi(y,N)=N^{-\gamma/\nu} * f(N^{1/\nu}(y-y_c)^{\gamma/\nu})$ where f , γ and ν are unknown and N is the number of spatial sites. If $y=y_c$ then $\chi(y,N)*N^{\gamma/\nu}=f(0)$. This is significant since this means that at the critical point, y_c , the function $\chi(y,N)*N^{\gamma/\nu}$ is independent of N . So if $\chi(y,N)*N^{\gamma/\nu}$ is plotted for a number of different lattice sizes on the same graph, the plots should cross at the critical point. Preliminary results look promising as illustrated in figures 7 and 8. Figure 7 shows plots for $N=4, 8, 16$ and 32 of χ_{CDW} before finite size scaling and figure 8 demonstrates the graphs after being multiplied by N^{-1} .

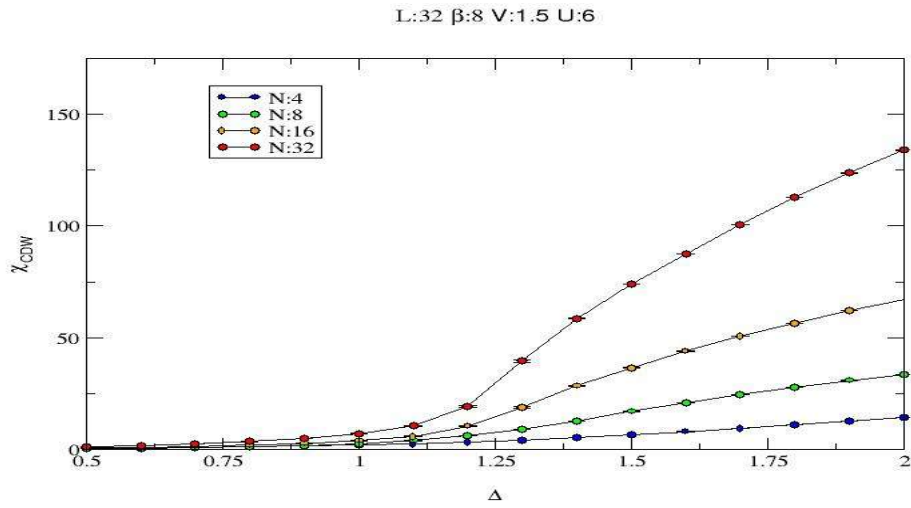


Figure Number range Figure CDW susceptibility for extended Hubbard model with staggered potential for $N=4, 8, 16, 32$ (before finite size scaling)

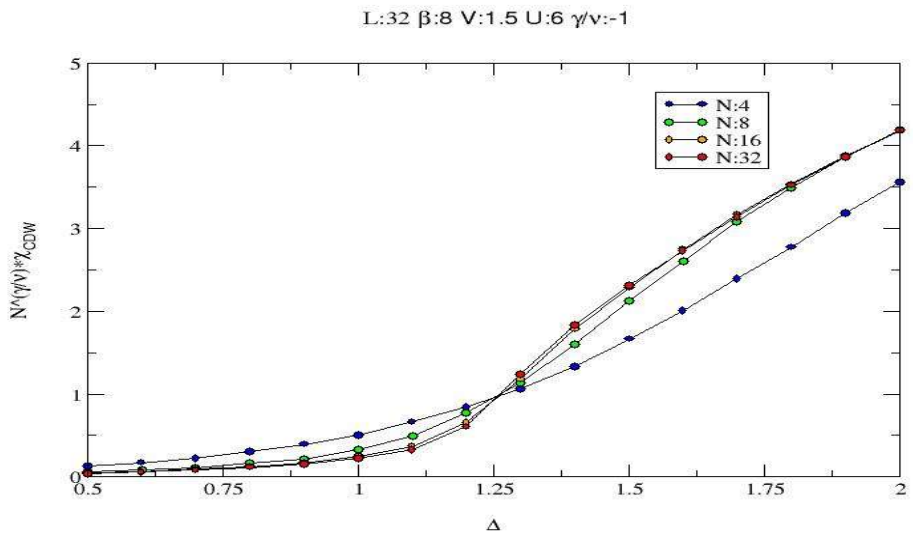


Figure Number range Figure Finite size scaling of the CDW susceptibility on the extended Hubbard model with staggered potential for $N=4, 8, 16, 32$

The energy of the phonons in the Hubbard-Holstein model can be solved exactly if no electrons are in the system (or if the el-ph coupling is set to zero). In addition, due to the properties of the harmonic oscillator, the kinetic energy of the phonons should al-

ways equal the potential energy. The energy is given by $E = \omega / (e^{\omega \beta} - 1) + \omega / 2$. figure 9 and 10. both illustrate the accuracy of the WLQMC code by plotting both the results from the program and the actual energy.

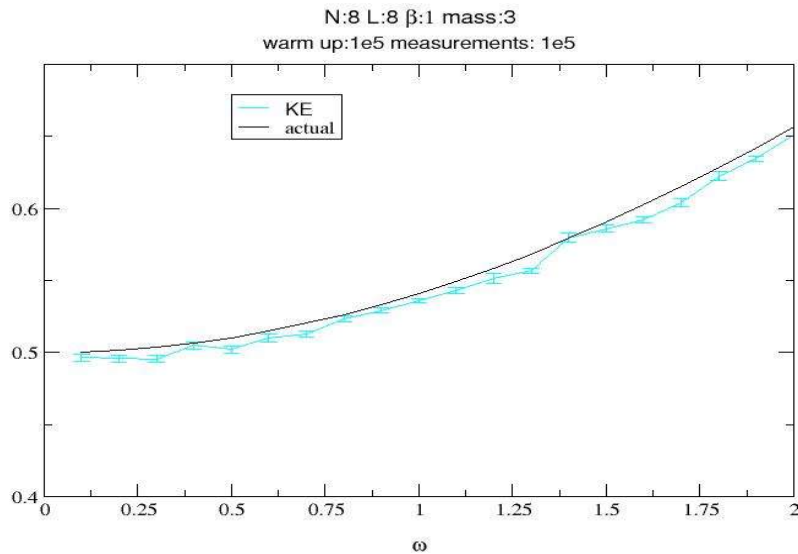


Figure Number range Figure WLQMC vs. actual: KE of the Holstein model

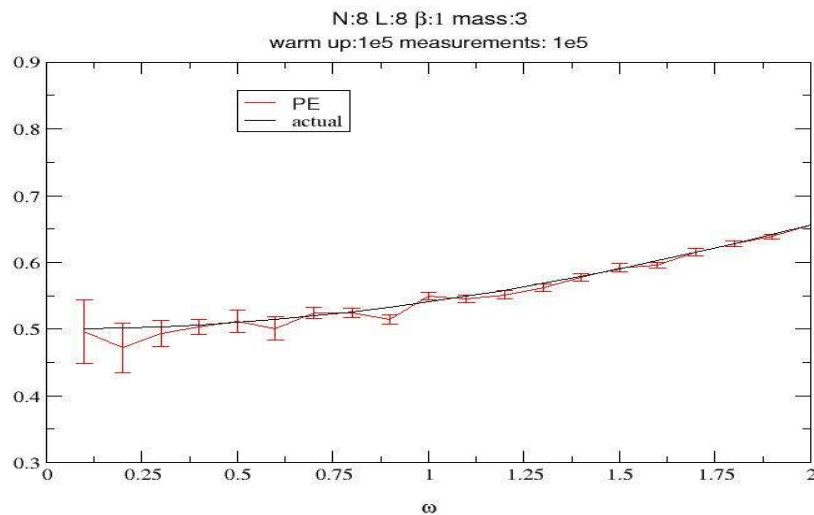


Figure Number range Figure WLQMC vs. actual: PE of the Holstein model

Additionally, if the kinetic energy has an ω of zero, this energy can be simplified so that the term $\omega/2$ disappears so that $KE = \omega/[2(e^{\omega\beta} - 1)]$. The expansion of e^x is given by $x^0/0! + x^1/1! + x^2/2! + \dots$. This expansion allows KE to be simplified to $\omega/[2(\omega\beta + (\omega\beta)^2/2! + \dots)] = 1/[2(\beta + \omega(\beta)^2/2! + \dots)]$ and if ω of zero, $KE = 1/(2\beta)$. This property of the kinetic energy was confirmed by the Monte Carlo program and is evident in figure 11.

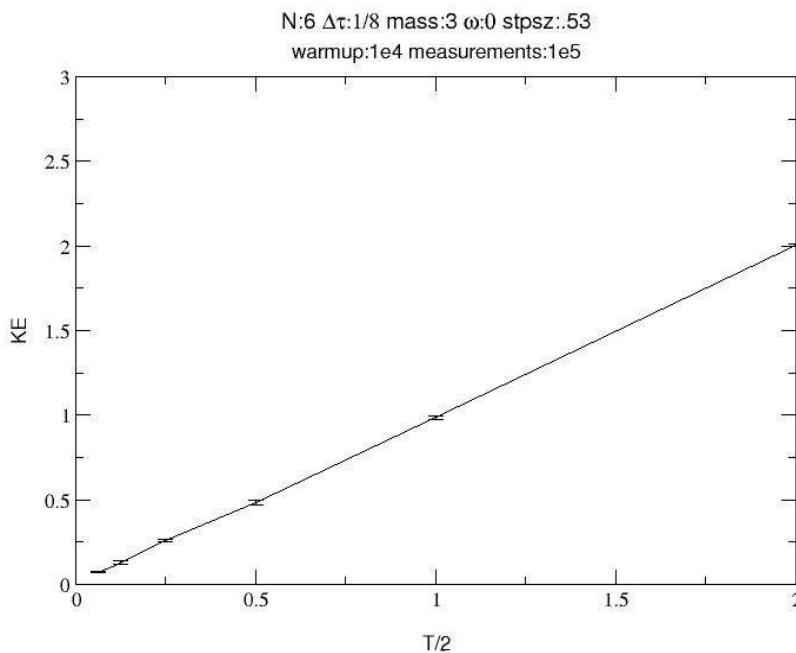


Figure Number range Figure The linear relationship of KE and T/2 for the Holstein model at $\omega=0$

When both phonons and electrons were included in the system, and the el-ph coupling was turned on, the results were very much similar to those produced by the staggered potential. As the electron-phonon coupling was turned on and increased, the charge density wave was increased while, conversely, the spin density wave was killed

off. This is best illustrated by the susceptibility of the charge density wave and spin density wave as illustrated in figures 12 and 13.

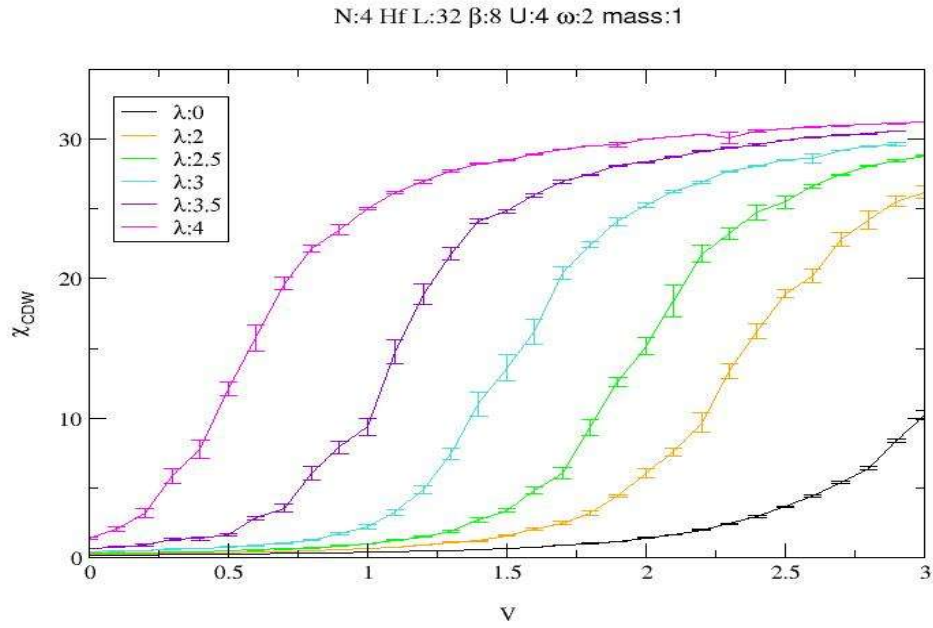


Figure Number range Figure CDW susceptibility for the extended Hubbard-Holstein model using $\lambda=0, 2, 2.5, 3, 3.5, 4$

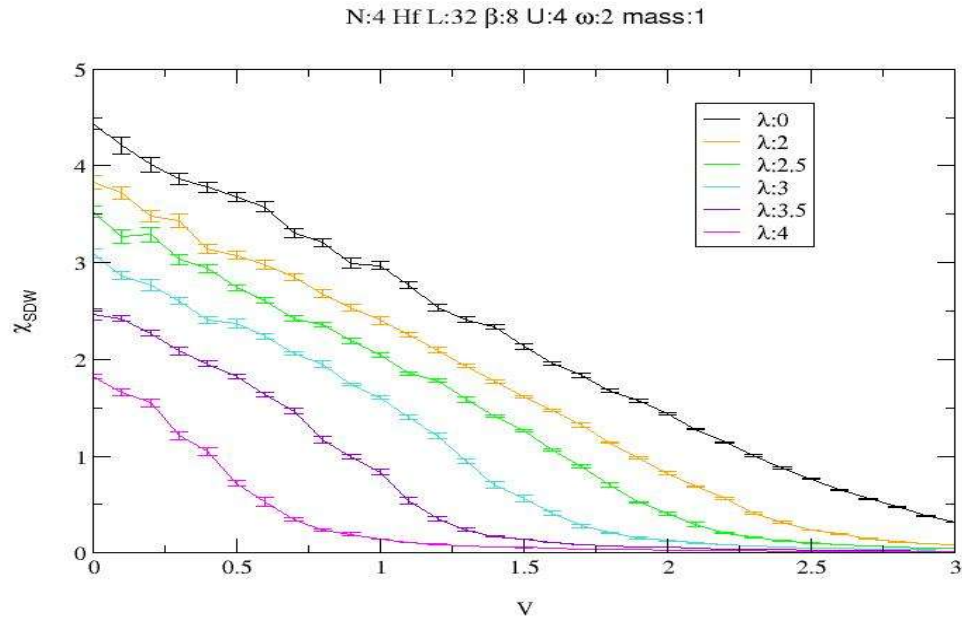


Figure Number range Figure SDW susceptibility for the extended Hubbard-Holstein model using $\lambda=0, 2, 2.5, 3, 3.5, 4$

CONCLUSION / FUTURE WORK

There is yet much more work to be done to study the Hubbard-Holstein model and the Hubbard model with staggered potential. Although ample testing has been completed to the WLQMC programs this summer, the actual phase diagrams of $U, V,$ and Δ and of $U, V,$ and λ have yet to be rendered. This is not exactly detrimental, but is simply a sign of interesting work yet to come. Further, preliminary results have shown themselves to be very encouraging for both our model and our method. From the work that has been completed this summer, we can conclude that the CDW phase is encouraged as Δ and λ are increased while the SDW is repressed. Future work that is vital to the fulfillment of the phase diagram will include utilizing larger lattices both for more realistic simulations and to employ the finite size scaling method; executing runs with larger β for

temperatures lower than room temperature; and having larger measurement period so as to reduce the amount of error in the data.